**Supplementary Table 6.** Continued

| Reference position | Gene | Chromosome | Coding sequence | Coverage | Allele change | Patient no. |
|---|---|---|---|---|---|---|
| 2162358340 | C14orf133 | 14 | 13 | 15 | delT | 1 |
| 2243652079 | NR2E3 | 15 | 6 | 129 | delC | 4 |
| 2256057594 | ADAMTSL3 | 15 | 12 | 26 | delT | 1 |
| 2277509768[a] | NLRC3 | 16 | 7 | 12 | delG | 2 |
| 2302633200 | EIF3C | 16 | 4 | 18 | delG | 4 |
| 2303380808 | SULT1A4 | 16 | 3 | 24 | delA | 1 |
| 2351412465 | LOC100289580 | 16 | 2 | 103 | delC | 4 |
| 2356396572 | P2RX5 | 17 | 3 | 40 | delG | 4 |
| 2376621991 | SPAG5 | 17 | 3 | 13 | delC | 1 |
| 2386619109 | CCDC49 | 17 | 5 | 14 | delT | 1 |
| 2413869089 | APOH | 17 | 5 | 24 | delC | 1 |
| 2501962862 | ZNF516 | 18 | 2 | 29 | delG | 3 |
| 2507200605 | MUM1 | 19 | 8 | 36 | delG | 1 |
| 2538892348 | C19orf55 | 19 | 9 | 20 | delG | 2 |
| 2565046537 | UBOX5 | 20 | 2 | 15 | delG | 1 |
| 2587599923 | ZNF337 | 20 | 4 | 19 | delT | 1 |
| 2598525448 | ZHX3 | 20 | 1 | 19 | delT | 1 |
| 2625038622 | NRIP1 | 21 | 1 | 24 | delG | 1 |
| 2661518554 | FAM108A5 | 22 | 2 | 13 | delG | 3 |
| 2748277559 | SPIN2B | X | 1 | 13 | delG | 2 |
| 2792445004 | TEX13A | X | 2 | 18 | delC | 3 |

[a]These indels commonly occurred in more than one HCC.

**Supplementary Table 7.** List of 40 Somatic Mutations With Amino Acid Changes Commonly Detected in Both the Tumor (at a Frequency of More Than 20% of Reads) and Matched Nontumorous Cirrhotic Liver (at a Frequency of More Than 5% of Reads) of the Same Patient

| | | | | | Tumor | | Nontumor | |
|---|---|---|---|---|---|---|---|---|
| Gene | Reference position | Chromosome | Reference nucleotide | Mutation nucleotide | Mutation frequency (%) | Patient no. | Mutation frequency (%) | Patient no. |
| LEPR | 65548341 | 1 | C | A | 25.8 | 3 | 15.0 | 3 |
| | | | | | | | 21.9 | 1 |
| ZNF408 | 1792629936 | 11 | T | A | 20.4 | 2 | 16.0 | 2 |
| | | | | | | | 15.8 | 4 |
| HRNR | 129676984 | 1 | G | C | 28.9 | 3 | 5.4 | 3 |
| PXDN | 228577682 | 2 | G | C | 45.1 | 4 | 47.2 | 4 |
| POTEF | 353150970 | 2 | T | A | 41.8 | 4 | 31.0 | 4 |
| ALPP | 455451136 | 2 | C | T | 32.5 | 4 | 37.5 | 4 |
| GPR125 | 682521774 | 4 | C | A | 38.1 | 2 | 40.0 | 2 |
| HERC6 | 746068457 | 4 | T | A | 36.5 | 4 | 44.9 | 4 |
| EGFLAM | 886579974 | 5 | T | G | 23.3 | 3 | 5.3 | 3 |
| C4A | 1057829599 | 6 | T | G | 25.0 | 2 | 11.5 | 2 |
| WISP3 | 1134999625 | 6 | T | G | 43.3 | 4 | 64.3 | 4 |
| C7orf10 | 1234451360 | 7 | T | A | 25.0 | 3 | 8.3 | 3 |
| PVRIG | 1290339880 | 7 | C | T | 23.5 | 1 | 21.3 | 1 |
| MUC17 | 1291200140 | 7 | G | A | 21.2 | 4 | 12.5 | 4 |
| PLOD3 | 1291376235 | 7 | G | C | 48.2 | 4 | 51.7 | 4 |
| COL27A1 | 1589933932 | 9 | A | G | 56.8 | 4 | 54.6 | 4 |
| AGAP9 | 1658906463 | 10 | T | G | 36.7 | 4 | 16.2 | 4 |
| POLL | 1713935693 | 10 | G | T | 44.8 | 4 | 38.6 | 4 |
| MUC5AC | 1747183167 | 11 | G | A | 43.9 | 4 | 43.8 | 4 |
| MRGPRX3 | 1764064669 | 11 | T | C | 40.0 | 4 | 42.5 | 4 |
| TMEM133 | 1843211533 | 11 | A | C | 59.5 | 4 | 83.3 | 4 |
| TMEM123 | 1844621025 | 11 | G | A | 27.3 | 2 | 7.3 | 2 |
| TMPRSS4 | 1860336319 | 11 | C | T | 54.4 | 4 | 41.3 | 4 |
| DHRS4L2 | 2108914889 | 14 | G | T | 20.5 | 3 | 11.5 | 3 |
| GOLGA6C | 2247104814 | 15 | A | T | 21.7 | 4 | 9.6 | 4 |
| PRSS22 | 2276813235 | 16 | C | T | 50.0 | 4 | 36.7 | 4 |
| FAM38A | 2351390771 | 16 | C | T | 21.4 | 4 | 54.3 | 4 |
| GGT6 | 2357265990 | 17 | G | A | 92.3 | 4 | 41.7 | 4 |
| COX10 | 2366897810 | 17 | C | T | 55.2 | 4 | 36.3 | 4 |
| KIAA0100 | 2376657621 | 17 | A | C | 47.8 | 4 | 60.0 | 4 |
| TBC1D3B | 2384202011 | 17 | C | T | 63.0 | 4 | 27.4 | 4 |
| TBC1D3D | 2385938140 | 17 | A | G | 45.9 | 4 | 21.0 | 4 |
| ERBB2 | 2387531879 | 17 | A | G | 66.7 | 4 | 54.6 | 4 |
| CSH2 | 2411602334 | 17 | C | T | 90.9 | 4 | 79.5 | 4 |
| QRICH2 | 2423941144 | 17 | T | G | 50.0 | 4 | 60.4 | 4 |
| MOCOS | 2461870479 | 18 | T | C | 72.0 | 4 | 62.2 | 4 |
| CPAMD8 | 2522819358 | 19 | G | A | 21.8 | 3 | 15.2 | 3 |
| MAP4K1 | 2541732174 | 19 | G | A | 36.0 | 4 | 54.3 | 4 |
| PSG8 | 2545901763 | 19 | C | A | 28.3 | 3 | 9.5 | 3 |
| KRTAP12-2 | 2654734983 | 21 | C | T | 59.3 | 4 | 43.5 | 4 |

NOTE. The first 2 genes listed were recurrently mutated in the nontumorous inflamed livers of 2 patients.

**Supplementary Table 8.** Overview of Selected Exome Sequencing Data From 22 Patients With HCV Infection

| | | Aligned reads | Aligned sequence (*base pairs*) | Median read depth |
|---|---|---|---|---|
| *TP53* | Tumor | 29,334 | 2,035,570 | 1476.2 |
| | Nontumor | 31,848 | 2,200,641 | 1575.3 |
| | Lymphocytes | 36,690 | 2,539,944 | 1917.2 |
| *CTNNB1* | Tumor | 90,022 | 6,215,000 | 2344.3 |
| | Nontumor | 75,785 | 5,282,450 | 1991.2 |
| | Lymphocytes | 100,430 | 7,013,325 | 2710.8 |
| *LEPR* | Tumor | 34,328 | 2,390,335 | 538.3 |
| | Nontumor | 60,128 | 4,219,089 | 1025.6 |
| | Lymphocytes | 86,830 | 6,085,511 | 1423.0 |

NOTE. Selected exome sequencing of *TP53*, *CTNNB1*, and *LEPR* was performed for 22 nontumorous cirrhotic liver tissues, 10 HCC tissues, and matched peripheral lymphocytes from each patient. Aligned reads, aligned sequences (base pairs), and median read depth are shown for each sample.

**Supplementary Table 9.** Clinical Features and Overview of Deep Sequencing Data of Patients Who Underwent Deep Sequencing of the *LEPR* Gene

| | Chronic hepatitis (n = 15) | Normal liver (n = 9) |
|---|---|---|
| Age (*y*) | 59.3 | 55.9 |
| Sex (male/female) | 6/9 | 7/2 |
| Aligned reads | 4290 | 3956 |
| Aligned sequence (*base pairs*) | 1,044,737 | 1,275,068 |
| Median read depth | 2838 | 3440 |
| No. of mutations in the *LEPR* gene | 0 | 0 |

NOTE. We determined the sequences of the *LEPR* gene in the liver of 15 noncirrhotic patients with HCV-associated chronic hepatitis. In addition, normal liver tissues were obtained from 9 liver donors at the time of the operation. Age, sex, aligned reads, aligned sequences (base pairs), median read depth, and numbers of mutations are shown.

**Supplementary Table 10.** Mean Body Weights and Serum Levels of Insulin, Triglyceride, Total Cholesterol, and Alanine Aminotransferase of C57BL/KsJ-*db/db* (*db/db*) Mice and Misty (Control) Mice After 4 Weeks of Treatment With TAA

| | *db/db* | Control |
|---|---|---|
| Body weight (*g*) | 46.5 ± 0.6 | 23.5 ± 0.4 |
| Insulin (*ng/mL*) | 30.6 ± 28.3 | 1.6 ± 0.2 |
| Triglyceride (*mg/dL*) | 95.0 ± 5.0 | 50.0 ± 20.0 |
| Total cholesterol (*mg/dL*) | 215.0 ± 15.0 | 95.0 ± 15.0 |
| Alanine aminotransferase (*IU/L*) | 1325.0 ± 1085.0 | 75.0 ± 35.0 |

NOTE. All data are presented as mean ± SD.

**Supplementary Table 11.** Categorization of the Mutated Genes Detected by Whole Exome Sequencing of the AID-Expressing Hepatocyte Cell Line Using the Kyoto Encyclopedia of Genes and Genomes Database

| Pathway | | | | |
|---|---|---|---|---|
| Metabolic pathways | ATP6V0A4 | DMGDH | HSD17B3 | PGD |
| | ATP6V1C2 | GALNT1 | HYAL2 | PHGDH |
| | BCMO1 | GATM | NDST1 | POLR3B |
| | CPS1 | HKDC1 | PAH | |
| PI3K-Akt signaling pathway | BCL2L11 | IBSP NOS3 | PRKCZ | TEK |
| | COL27A1 | | | |
| MAPK signaling pathway | FLNB | SP1 | CACNA1F | PTPN7 |
| Cytokine-cytokine receptor interaction | LEPR | TNFRSF8 | TNFRSF10A | |
| Transcriptional misregulation in cancer | EYA1 | GZMB | JMJD7-PLA2G4B | |
| Proteoglycans in cancer | FLN | ITGB3 | TIMP3 | VTN |
| PPAR signaling pathway | CPT1B | CYP4A22 | PPARD | |
| Cell cycle | E2F2 | ESPL1 | MCM7 | |
| Pathways in cancer | FLT3 | TRAF4 | PDGFA | |
| Hedgehog signaling pathway | GLI3 | LRP2 | CSNK1A1L | |
| Others | 95 genes | | | |

NOTE. The genes categorized in multiple pathways are shown in only one representative pathway. Constitutive AID expression resulted in the accumulation of nucleotide alterations in various genes, including LEPR, of the cultured hepatocyte–derived cells. Whole exome sequencing was performed on DNA derived from established non-neoplastic human primary hepatocyte cells[6] with constitutive AID expression. AID expression in the cultured hepatocytes was performed using a lentiviral system.[5] After 8 weeks of AID expression, the DNA was extracted and subjected to whole exome sequencing as described in Materials and Methods. Overall, a total of 460 nucleotide positions in 380 different genes were defined as mutated in the AID-expressing cultured hepatocytes through the variant filtering process. Among them, pathway analyses by the Kyoto Encyclopedia of Genes and Genomes revealed that many genes, including LEPR, were categorized into well-known signaling pathways: the metabolic pathway, PI3K-Akt signaling pathway, MAPK signaling pathway, cytokine-cytokine receptor interaction pathway, and transcriptional misregulation in cancer pathway. Only categorized genes are shown.

Lasers Med Sci (2015) 30:383–387
DOI 10.1007/s10103-014-1681-6

ORIGINAL ARTICLE

# Antimicrobial action from a novel porphyrin derivative in photodynamic antimicrobial chemotherapy in vitro

**Miftahul Akhyar Latief · Taiichiro Chikama · Momoko Shibasaki · Takaaki Sasaki · Ji-Ae Ko · Yoshiaki Kiuchi · Takemasa Sakaguchi · Akira Obana**

Received: 19 May 2014 / Accepted: 17 October 2014 / Published online: 30 October 2014


**Abstract** Efforts to identify improved treatments for corneal infection include the development of photodynamic antimicrobial chemotherapy (PACT). We evaluated the antimicrobial effect of PACT with a novel porphyrin derivative, TONS 504, and a novel light system on methicillin-sensitive *Staphylococcus aureus* (MSSA) and methicillin-resistant *Staphylococcus aureus* (MRSA). Bacteria were irradiated with a light-emitting diode (LED) at energies of 10, 20, or 30 J/cm$^2$ in the presence of various concentrations of TONS 504. Bacterial viability was assessed at 30 min and 24 h after irradiation by determination of colony formation on agar plates. PACT inhibited the growth of both MSSA and MRSA as early as 30 min after light exposure. Complete inhibition of bacterial growth was apparent at 24 h after irradiation at a TONS 504 concentration of 1 mg/L and LED energies of ≥10 J/cm$^2$ or a TONS 504 concentration of 0.5 mg/L and LED energies of ≥20 J/cm$^2$ for MSSA, and at a TONS 504 concentration of 10 mg/L and LED energies of ≥10 J/cm$^2$ or of a TONS 504 concentration of 1 mg/L and LED energies of ≥20 J/cm$^2$ for MRSA. Bacterial growth was unaffected by TONS 504 in the absence of irradiation or by irradiation in the absence of TONS 504. Our results thus demonstrate the antimicrobial efficacy of PACT with TONS 504 and a LED against both MSSA and MRSA in vitro, and they therefore provide a basis for further investigation of this system as a potential treatment for corneal infection.

**Keywords** PACT · Porphyrin · MSSA · MRSA

M. A. Latief · T. Chikama (✉) · M. Shibasaki · T. Sasaki · J.-A. Ko · Y. Kiuchi
Department of Ophthalmology and Visual Science, Graduate School of Biomedical Sciences, Hiroshima University, 1-2-3 Kasumi, Minami-Ku, Hiroshima 734-8551, Japan
e-mail: chikama@hiroshima-u.ac.jp

M. A. Latief
Medical Faculty, Muhammadiyah University, Makassar City 90221, South Sulawesi, Indonesia

M. A. Latief
Department of Ophthalmology, Hasanuddin University, Makassar City 90245, South Sulawesi, Indonesia

T. Sakaguchi
Department of Virology, Graduate School of Biomedical Sciences, Hiroshima University, Hiroshima 734-8551, Japan

A. Obana
Department of Ophthalmology, Seirei Hamamatsu General Hospital, Shizuoka 430-8558, Japan

## Introduction

Corneal diseases, and in particular corneal infection, are a major cause of blindness worldwide [1]. Corneal infection and associated inflammation can lead to corneal scarring [1], and they present a challenge to treatment. Efforts to find effective treatments to eradicate microorganisms have included the development of photodynamic therapy. A photodynamic effect occurs when photosensitizer molecules absorb light and then dissipate the absorbed energy by transferring it to biological acceptors (usually oxygen), thereby generating an excess of reactive species that force cells into death pathways. The concept of photodynamic therapy as a treatment modality to eradicate microorganisms has been around for more than a century [2–8].

Porphyrins constitute a group of macrocyclic photosensitizers that have been tested and applied widely against Gram-positive and Gram-negative bacteria. The discovery of many novel photosensitizers that function in combination with specific wavelengths of light has revealed that cationic and hydrophilic photosensitizers are more effective as antimicrobial agents than are anionic and hydrophobic ones [2].

In an attempt to develop a new treatment for corneal infection, we have now evaluated the effectiveness of photodynamic antimicrobial chemotherapy (PACT) with a novel porphyrin derivative (TONS 504) and a light irradiation system based on a light-emitting diode (LED) against the Gram-positive bacterium methicillin-sensitive *Staphylococcus aureus* (MSSA) as well as methicillin-resistant *Staphylococcus aureus* (MRSA) in vitro. Since this study was our first step for establishment of a new treatment for corneal infection, we focused to evaluate the efficacy of TONS 504-PACT in vitro against MSSA and MRSA as familiar bacteria in corneal infection in this time. Whereas PACT for the ubiquitous species MSSA has been studied with photosensitizers such as hematoporphyrin, phthalocyanine, 5-aminolaevulinic acid, and photofrin [9], the effectiveness of the novel porphyrin derivative TONS 504 against both MSSA and MRSA has not previously been examined. Furthermore, we have used a LED for PACT with TONS 504. Although such a LED has previously been studied and applied as a light source for PACT in vitro [5], we applied settings that yield different light energies and a short irradiation time.

## Materials and methods

### Microorganisms

A strain of MSSA obtained from NITE Biological Resource Center (NBRC 13276) and a strain of MRSA obtained from Eiken Chemical Co. Ltd. (ENK 1122) and kindly provided by the Clinical Laboratory of Hiroshima University Hospital were grown in Mueller Hinton broth. Each bacterium was transferred aseptically into 15 mL of fresh medium and maintained overnight at 37 °C in a shaking incubator. The cells were harvested by centrifugation (3000×*g* for 10 min at −4 °C), washed three times with Mueller Hinton broth, and suspended in phosphate-buffered saline to an optical density at 600 nm of 0.950 to 1.050, which corresponds to ~$1\times10^7$ colony-forming units (CFU)/mL for each microorganism [10, 11] for use as a standard preparation.

### The photosensitizer

TONS 504 [13,17-bis (1-carboxyethyl) carbamoyl (3-methylpyridine)-3-(1,3-dioxane-2-yl) methylidene-8-ethenyl-2-hydroxy-2,7,12,18-tetramethyl chlorin, diN-methy iodide ($C_{51}H_{58}O_5I_2$)], a hydrophilic and cationic porphyrin derivative with a greenish color and molecular weight of 1116.9 (Fig. 1), was purchased from Porphyrin Laboratory (Okayama, Japan). At first, we tried to confirm the effectiveness of TONS 504 as a photosensitizer combined with the LED light irradiation against MSSA. Then, we decided to continue this study using TONS 504 as the photosensitizer. For experiments, TONS 504 was dissolved in sterile double-distilled water and serially diluted with Mueller Hinton broth to the desired concentrations (0.01 to 10 mg/L). The color of the dilutions was almost identical to that of Mueller Hinton broth, with the exception of the concentration of 10 mg/L, for which the color was a subtle green-yellow. However, the bottom of culture wells containing all dilutions was clearly visible.

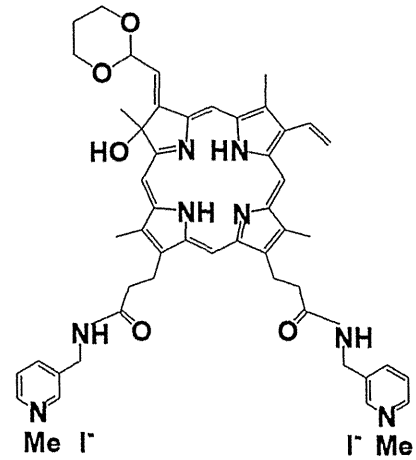


Fig. 1 Chemical structure of the novel cationic porphyrin derivative TONS 504

### LED system

A LED system that provides a single light beam with a specific wavelength of 660 nm was obtained from CCS Inc. (Kyoto, Japan). The LED power was measured with an optical power meter (Hioki, Nagano, Japan) during each experiment. The increase in temperature conferred by the LED device was measured with a wire thermometer placed inside the wells of the culture plate during irradiation. We found that irradiation at a distance of 5 cm from the light source to the bottom of the plate yielded a light energy of 10 J/cm$^2$ over 3 min. On the basis of the temperature measurements, we included a 1-min rest period between each 3-min light exposure in order to avoid a problematic increase in temperature (data not shown).

### PACT

We evaluated the effects of TONS 504 on MSSA and MRSA without LED exposure, the effects of LED exposure in the absence of TONS 504, and the effects of the combination of TONS 504 and LED exposure (TONS 504–PACT) at 10, 20, or 30 J/cm$^2$. The bacteria ($1\times10^7$ CFU/mL) were plated in

each well of a 24-well plate; TONS 504 was added to the wells at various concentrations, and the plate was incubated for 5 min before exposure to the LED at 10 J/cm$^2$ (single 3-min exposure), 20 J/cm$^2$ (two 3-min exposures separated by a 1-min rest period), or 30 J/cm$^2$ (three 3-min exposures with two 1-min rest periods). We evaluated the effects of TONS 504–PACT at 30 min and 24 h after irradiation and incubation of the plate at 37 °C. At 30 min, 100 μL of the contents of each well were transferred to an agar plate (diameter, 10 cm). The 24-well plate was then returned to the 37 °C incubator. At 24 h, the wells were inspected for proliferation of the microorganisms as evident by the turbidity of the medium (Figs. 2 and 3). The inspection of the turbidity of the medium, however, is a relatively new method which we aim to share. It is an easy and quick method to suggest whether the microorganisms are in a good condition to proliferate or not. Surely, then all of the wells regardless clear or not, should be confirmed by checking the viability of microorganisms, which was evaluated further by the transfer of 100 μL of the contents of each well to an agar plate. The solid medium consisted of a combination of polypeptone (Nihon Pharmaceutical Co. Ltd., Tokyo, Japan), dried yeast extract, magnesium sulfate heptahydrate, and agar (Nacalai Tesque, Kyoto, Japan) with the pH set to 7.0. The agar plates were incubated for 1 to 3 days at 37 °C, after which visible colonies were counted. The number of colonies formed (0 to 300 per plate) was within the range of detectable colony formation.

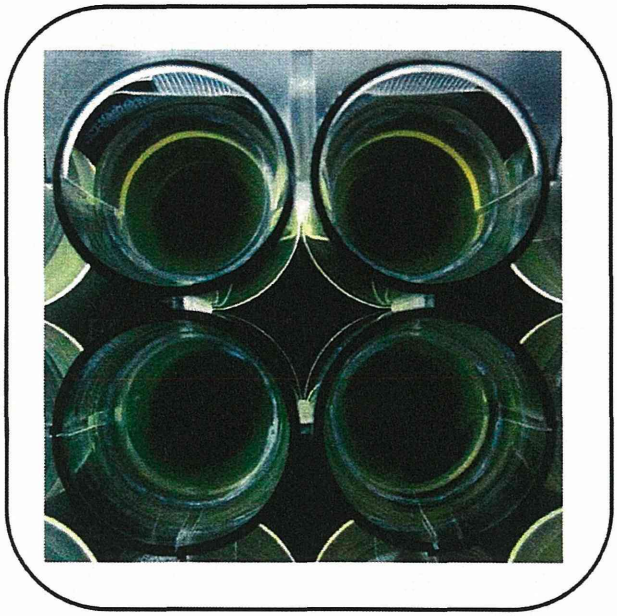

**Fig. 2** Visual assessment of the antimicrobial action of TONS 504–PACT on the basis of medium turbidity. Bacteria were plated in 24-well plates, exposed to TONS 504, irradiated with a LED, and incubated for 24 h at 37 °C. Examples of wells in which bacterial proliferation was evident from the high turbidity of the medium are shown

**Fig. 3** Visual assessment of the antimicrobial action of TONS 504–PACT on the basis of medium turbidity. Bacteria were plated in 24-well plates, exposed to TONS 504, irradiated with a LED, and incubated for 24 h at 37 °C. Examples of wells in which the clarity of the medium was indicative of no bacterial growth are shown

## Results

### Antimicrobial effect of TONS 504–PACT on MSSA

PACT with TONS 504 as the photosensitizer and a LED as the light source resulted in a reduction in the viability of MSSA in a manner dependent on both LED energy and TONS 504 concentration (Table 1). The antimicrobial effect was apparent both visually at 24 h after LED irradiation and after subsequent measurement of colony formation on agar plates. For MSSA irradiated at 10 J/cm$^2$, the antimicrobial effect of TONS 504 was complete at a concentration of 1 mg/L, whereas for bacteria irradiated at 20 or 30 J/cm$^2$, the antimicrobial effect was complete at a TONS 504 concentration of 0.5 mg/L. Furthermore, inhibition of bacterial growth by TONS 504–PACT was also apparent as early as 30 min after irradiation. Suspensions of MSSA either treated with TONS 504 but not irradiated or irradiated in the absence of TONS 504 did not show a reduction in viability.

### Antimicrobial effect of TONS 504–PACT on MRSA

PACT with TONS 504 also reduced the viability of MRSA in a manner dependent on both LED energy and TONS 504 concentration (Table 2). The antimicrobial effect was again

**Table 1** Antimicrobial effect of TONS 504–PACT on MSSA

| Time | LED energy (J/cm$^2$) | TONS 504 (mg/L) | | | | | |
|---|---|---|---|---|---|---|---|
| | | 0 | 0.01 | 0.1 | 0.5 | 1 | 10 |
| 30 min | 0 | >300 | >300 | >300 | >300 | >300 | >300 |
| | 10 | >300 | >300 | >300 | >300 | 24.5±10.3 | 1.75±1.0 |
| | 20 | >300 | >300 | >300 | >300 | 12.2±13.3 | 2.25±2.9 |
| | 30 | >300 | >300 | >300 | >300 | 21.5±18.8 | 1.25±1.3 |
| 24 h | 0 | >300 | >300 | >300 | >300 | >300 | >300 |
| | 10 | >300 | >300 | >300 | >300 | 0 | 0 |
| | 20 | >300 | >300 | >300 | 0 | 0 | 0 |
| | 30 | >300 | >300 | >300 | 0 | 0 | 0 |

Data represent colony number per agar plate and are means±SD for four independent experiments each performed in triplicate

apparent both visually at 24 h after LED irradiation and after subsequent measurement of colony formation on agar plates. For MRSA irradiated at 10 J/cm$^2$, the antimicrobial effect of TONS 504 was complete at a concentration of 10 mg/L. At a light energy of 20 or 30 J/cm$^2$, the antimicrobial effect of TONS 504 was absolute at 1 mg/L. Furthermore, inhibition of bacterial growth by TONS 504–PACT was also apparent as early as 30 min after irradiation. Again, suspensions of MRSA either treated with TONS 504 but not irradiated or irradiated in the absence of TONS 504 did not show a reduction in viability.

## Discussion

We have developed a PACT system based on a novel porphyrin derivative (TONS 504) as a photosensitizer and a LED-based irradiation approach with a single light beam of 660 nm. This system inhibited the proliferation of MSSA and MRSA in vitro with high potency and efficacy. No such effect was apparent after exposure of the bacteria either to TONS 504 in the absence of irradiation or to light in the absence of the photosensitizer.

Porphyrin and its derivatives have been widely used as photosensitizers for photodynamic therapy [2]. The porphyrin derivative chlorin e6 in combination with a LED light source with a wavelength of 664 nm was found to be effective against MSSA, *Pseudomonas aeruginosa*, *Escherichia coli*, and *Salmonella enterica* serovar *Typhimurium* [10]. The combination of chlorin e6 and a helium-neon laser was also effective against several strains of MSSA and MRSA [11]. Another study demonstrated the antimicrobial effect of the combination of chlorin e6 and a LED with a wavelength of 662 nm against 12 types of oral pathogen [12]. We have now shown the efficacy of PACT with a new photosensitizer (TONS 504) combined with a low energy of LED-based irradiation system.

The inhibitory effects of TONS 504–PACT on MSSA and MRSA in the present study were apparent both visually after culture of the cells for 24 h in 24-well plates as well as by subsequent determination of colony number after plating of the treated cells on agar. The antimicrobial effects of TONS 504–PACT were also apparent, but not yet complete, as early as 30 min after LED irradiation. This rapid action of TONS

**Table 2** Antimicrobial effect of TONS 504–PACT on MRSA

| Time | LED energy (J/cm$^2$) | TONS 504 (mg/L) | | | | | |
|---|---|---|---|---|---|---|---|
| | | 0 | 0.01 | 0.1 | 0.5 | 1 | 10 |
| 30 min | 0 | >300 | >300 | >300 | >300 | >300 | >300 |
| | 10 | >300 | >300 | >300 | >300 | >300 | >300 |
| | 20 | >300 | >300 | >300 | >300 | 212.5±12.2 | 127.8±17.8 |
| | 30 | >300 | >300 | >300 | >300 | 292±10.9 | 106.8±5.6 |
| 24 h | 0 | >300 | >300 | >300 | >300 | >300 | >300 |
| | 10 | >300 | >300 | >300 | >300 | >300 | 0 |
| | 20 | >300 | >300 | >300 | >300 | 0 | 0 |
| | 30 | >300 | >300 | >300 | >300 | 0 | 0 |

Data represent colony number per agar plate and are means±SD for four independent experiments each performed in triplicate

504–PACT is consistent with the proposed mechanism of photodynamic therapy [2–4, 8]. The photosensitizer is not necessarily destroyed after irradiation; it can return to its ground state by phosphorescence without chemical alteration and may be able to repeat the process of energy transfer many times. We found that, at a light energy of 20 or 30 J/cm$^2$, the growth of MSSA was completely inhibited at 24 h after irradiation in the presence of TONS 504 at concentrations of 0.5, 1, and 10 mg/L whereas that of MRSA was similarly blocked at TONS 504 concentrations of 1 and 10 mg/L. A light energy of 20 J/cm$^2$ and a TONS 504 concentration of 1 mg/L thus appear to be sufficient to inhibit the proliferation of both microorganisms completely.

On the basis of our results, further study is warranted to determine the effects of TONS 504–PACT. Our demonstration of the antimicrobial action of low concentrations of a novel cationic porphyrin derivative combined with low light energies is consistent with the results of a previous study showing a cationic photosensitizer to be more effective than an anionic agent in this regard [2, 13].

In conclusion, we have demonstrated the efficacy of PACT with the novel porphyrin derivative TONS 504 and a LED setup for the elimination of both MSSA and MRSA. We are now planning further investigation of this system as an antimicrobial treatment for other microorganisms including Gram-negative bacteria, fungi, viruses, and parasites both in vitro and in vivo. Furthermore, clinical study should be considered regarding the results as an address for the treatment of corneal infection.

**Acknowledgments** We thank Isao Sakata (Porphyrin Laboratory, Okayama, Japan) for providing information of TONS 504 as well as Akira Ichikawa (CCS Inc., Kyoto, Japan) for creating the LED device according to our experimental design.

**Funding** This work is supported by Adaptable and Seamless Technology transfer Program through target-driven R&D (A-STEP) of the Japan Science and Technology Agency (JST).

**Conflict of interest** The authors declare that they have no conflict of interest.

## References

1. Whitcher JP, Srinivasan M, Upadhyay MP (2001) Corneal blindness: a global perspective. Bull WHO 79:214–221
2. Wainwright M (1998) Photodynamic antimicrobial chemotherapy (PACT). J Antimicrob Chemother 42:13–28
3. Dougherty TJ, Gomer CJ, Henderson BW (1998) Photodynamic therapy. J Natl Cancer Inst 90:889–905
4. Pass HI (1993) Photodynamic therapy in oncology: mechanisms and clinical use. J Natl Cancer Inst 85:443–456
5. Calin MA, Parasca SV (2009) Light sources for photodynamic inactivation of bacteria. Lasers Med Sci 24:453–460
6. Nitzan Y, Shainberg B, Malik Z (1989) The mechanism of photodynamic inactivation of *MSSA* by deuteroporphyrin. Curr Microbiol 19: 265–269
7. Plaetzer K, Krammer B, Berlanda J, Berr F, Kiesslich T (2009) Photophysics and photochemistry of photodynamic therapy: fundamental aspects. Lasers Med Sci 24:259–268
8. Donnelly RF, McCarron PA, Woolfson D (2009) Drug delivery systems for photodynamic therapy. Recent Patents Drug Deliv Formul 3:1–7
9. Wood S, Metcalf D, Devine D, Robinson C (2006) Erythrosine is a potential photosensitizer for the photodynamic therapy of oral plaque biofilms. J Antimicrob Chemother 57:680–684
10. Park JH, Moon YH, Bang IS, Kim YC, Kim SA, Ahn SG, Yoon JH (2010) Antimicrobial effect of photodynamic therapy using a highly pure chlorin e6. Lasers Med Sci 25:705–710
11. Embleton ML, Nair SP, Cookson BD, Wilson M (2002) Selective lethal photosensitization of methicillin-resistant *MSSA* using an IgG-tin (IV) chlorin e6 conjugate. J Antimicrob Chemother 50:857–864
12. Rovaldi CR, Pievsky A, Sole NA, Friden PM, Rothstein DM, Spacciapoli P (2000) Photoactive porphyrin derivative with broad-spectrum activity against oral pathogens in vitro. Antimicrob Agents Chemother 44:3364–3367
13. Gois MM, Kurachi C, Santana EJB, Mima EGO, Spolidorio DMP, Pelino JEP, Bagnato VS (2009) Susceptibility of *Staphylococcus aureus* to porphyrin-mediated photodynamic antimicrobial chemotherapy: an in vitro study. Lasers Med Sci 25:391–395

# 柿渋でウイルス対策
# 柿タンニンによる強力なウイルス不活化作用

# A novel anti-Norovirus preventive measure: Efficient inactivation of pathogenic viruses by plant-derived tannins including persimmon (*Diospyros kaki*) tannin.

坂口 剛正（*SAKAGUSHI Takemasa*）* 上田 恭子（*UEDA Kyoko*）* 川端 涼子（*KAWABATA Ryoko*）*

* 広島大学大学院医歯薬保健学研究院ウイルス学

Key Words：柿タンニン・抗ウイルス作用・作用機序・インフルエンザウイルス・ノロウイルス
Key Words：persimmon; anti-viral; protein aggregation; influenza virus; feline calicivirus; mouse norovirus

**Abstract.**

Tannins, plant-derived polyphenols and other related compounds, have been utilized in many fields such as the food industry and manufacturing. In this study, we investigated the anti-viral effects of persimmon (*Diospyros kaki*) -derived tannin as well as other tannins such as those derived from green tea, acacia and gallnuts on 12 different viruses, which included surrogate viruses of human norovirus, feline calicivirus and mouse norovirus. Only persimmon tannin restricted viral infectivity in more than 4 log scale, showing strong anti-viral effects against a broad range of viruses. Other tannins were effective for some or none of the viruses. We then investigated the mechanism of the anti-viral effects of persimmon tannin, and found that viral protein aggregation with persimmon tannin seems to be a fundamental mechanism. Considering that persimmon tannin is a food supplement, it has a potential to be utilized as a safe and highly effective anti-viral reagent against human norovirus and other pathogenic viruses.

## はじめに

渋柿の抽出物あるいはそれを発酵させた”柿渋”は，防腐効果や強度を増すための塗料として，漁網，釣り糸，木造建築の下塗り，うちわや和傘などの工芸品に使われてきた。また，布の染色（柿渋染め）や民間薬，清酒を醸造する際の清澄剤としても用いられ，日本人に広く親しまれてきた。柿渋については，欧米ではあまり情報がなく，主にアジア中心に使われているようである。柿渋の主成分の柿タンニンには，

*To whom correspondence should be addressed.
Department of Virology, Institute of Biomedical & Health Sciences,
Hiroshima University, 1-2-3 Kasumi, Minami-ku, Hiroshima 734-8551, Japan
TEL：+81-82-257-5157 FAX：+81-82-257-5159 E-mail：tsaka@hiroshima-u.ac.jp

連絡先：〒734-8551 広島県広島市南区霞 1-2-3
広島大学大学院医歯薬保健学研究院ウイルス学
Tel：082-257-5157 Fax：082-257-5159 E-mail：tsaka@hiroshima-u.ac.jp

実際にいろいろな生理活性（蛋白質の凝集，抗微生物作用，抗酸化作用，抗腫瘍作用など）があることが科学的にも証明されている[1]。我々は，柿タンニンのウイルスに対する作用を調べて，どのウイルスも「不活化」してしまうという強力な抗ウイルス活性があることを見いだした[2]。

ウイルスは他の微生物と大きく異なり，DNAまたはRNAいずれかのウイルス遺伝子と，それを取り囲むカプシドと呼ばれるウイルス蛋白質の殻から構成される，いわば「さまよえる遺伝子」である[3]。ウイルスは細胞に感染して，宿主側の代謝酵素やリボソームなどの細胞の機能に依存して増殖する。細菌を殺すのは「殺菌」であるが，ウイルスの場合は，単なる物質（遺伝子）が細胞に入って活性化するのを防ぐという意味で，「不活化」と呼ぶ。

公衆衛生上，特に問題になっているのはヒトノロウイルスである。もともとカキなどの二枚貝の生食で発症することがよく知られていたが，二枚貝が関係しなくとも冬場の「お腹にくる風邪」の原因として，さらに食中毒の原因として広く認知されるようになった。学校給食や仕出し弁当が発生源になると大規模な集団感染がおこる。

ヒトノロウイルスは人間の腸でしか増殖しないが，便に大量に含まれ，症状が治まっても2週間前後，あるいは症状がなくても不顕性感染をおこしてウイルスを排泄することがある。一方で，1000ゲノムコピーで10%の人が発症するというボランティアを使った実験があるように[4]，ごく少量で感染・発症する。感染経路としては，ウイルスの付着した食品を摂取したり(経口感染)，手にウイルスをつけて口にもっていったり（接触感染)，ウイルスを含む微小水滴やほこりを吸い込むことで感染する（飛沫核感染，塵埃感染)。

ヒトノロウイルスは，一般に消毒しにくく，エタノールや逆性石けんはあまり効果がない。一般には次亜塩素酸ナトリウムが使用されるが，刺激性があり，皮膚などの人体に直接使うものではない。それゆえ，ヒトノロウイルスに適切な消毒剤が求められている。

## 1. 柿タンニンの抗ウイルス作用の検証

ウイルスは最外層に脂質二重膜（エンベロープ）をもつエンベロープウイルスと，これをもたない非エンベロープウイルスに分けられる。エンベロープはエタノールによって溶解するため，エンベロープウイルスはエタノールに高感受性である。一方，非エンベロープウイルスは概してエタノールに抵抗性であり，さらに他の消毒薬によっても不活化されにくい傾向がある。それぞれから6種類ずつ，12種類（表1）のウイルスを選んで試験に用いた。

エンベロープウイルスとして，インフルエンザウイルス（ヒト，鳥由来)，単純ヘルペスウイルス，水疱性口内炎ウイルス（牛，羊などに水疱性疾患をおこす)，センダイウイルス（げっ歯類に肺炎をおこす)，ニューカッスル病ウイルス（鳥類に感染する)，非エンベロープウイルスとして，ポリオウイルス（小児麻痺)，コクサッキーウイルス（手足口病，髄膜炎)，アデノウイルス（風邪，結膜炎など)，ロタウイルス（小児に下痢症を起こす）を用いた。問題となっているヒトノロウイルスは非エンベロープウイルスであるが，培養細胞で増殖しないために直接試験に用いることができない。その代替ウイルスとして，近縁であるネズミノロウイルス，ネコカリシウイルスを用いた（表1)。

柿タンニンとして，渋柿の絞り汁をいったん凍結乾燥したものを，10%エタノールに溶解して使用した。その他，比較のために，他の植物タンニンや同様の構造をもつ化合物を同濃度で用いた。緑茶タンニン（カテキンFP95緑茶抽

表1　タンニン類の抗ウイルス効果

| ウイルス | エンベロープ | タンニン類 | | | | | | |
|---|---|---|---|---|---|---|---|---|
| | | 柿タンニン | ワットルタンニン | コーヒータンニン | 緑茶タンニン | ペンタガロイルグルコース | プロピルガレート | ピロガロール |
| ヒトインフルエンザウイルス（H3N2） | ＋ | **5.8** | **5.7** | 0.7 | **5.8** | **4.8** | 1.8 | **5.8** |
| 鳥インフルエンザウイルス（H5N3） | ＋ | **6.2** | **6.1** | 0.7 | **6.2** | **5.1** | 2.3 | **6.2** |
| 単純ヘルペスウイルス | ＋ | **5.1** | **4.1** | 0.6 | **4.2** | **4.2** | 0.4 | **5.1** |
| 水疱性口内炎ウイルス | ＋ | **4.2** | 3.3 | 0.4 | **4.2** | 3.3 | 1.4 | **4.2** |
| センダイウイルス | ＋ | **6.6** | **6.0** | 0 | **6.2** | **6.1** | **5.1** | **6.0** |
| ニューカッスル病ウイルス | ＋ | **5.1** | **5.1** | 0 | **5.1** | **4.2** | 1.3 | 0.06 |
| ポリオウイルス | － | **5.4** | **4.5** | 0.09 | **5.4** | 3.6 | 0.03 | 0.6 |
| コクサッキーウイルス | － | **5.2** | 1.4 | 0.1 | 1.5 | 1.5 | 0 | 0.4 |
| アデノウイルス | － | **4.3** | 3.2 | 0.2 | 3.2 | 3.3 | 0.4 | 3.1 |
| ロタウイルス | － | **5.3** | **5.3** | 0.06 | **5.3** | **5.3** | **5.3** | **5.3** |
| ネコカリシウイルス | － | **4.9** | **4.9** | 0.05 | **4.1** | 3.9 | 0.3 | 0.1 |
| マウスノロウイルス | － | **4.3** | 1.6 | 0 | 1.7 | 0.9 | 0.2 | 0.4 |

タンニン処理による感染価の減少を対数で表しており，4以上（下線と太字で強調）はウイルス不活化効果があることを示す。

出物），ワットルタンニン（アカシアタンニン），コーヒータンニン（カフェノールP-100生コーヒー抽出物），ペンタガロイルグルコース（五倍子抽出・精製物），プロピルガレート（没食子酸プロピル），ピロガロール（焦性没食子酸）である。

試験方法は，ウイルスとタンニンを混合して（タンニンの終濃度は0.25%（w/v）），3分間以上，室温に置いて反応させてから稀釈して反応をとめ，ウイルスがどれくらい生き残っているかを調べた。元のウイルスの感染価（1 mlあたりの生きているウイルス数）が，タンニン処理によって10000分の1以下に低下すれば（すなわち，99.99%以上感染抑制，対数でいえば4以上の低下），その試薬はウイルスに対して有効であったと判定した。

鳥インフルエンザウイルス（H5N3）に対しては，柿タンニン，ワットルタンニン，緑茶タンニン，ペンタガロイルグルコース，ピロガロールの5種類のタンニンが有効であった（図1A）。一方，コクッサッキーウイルスに対しては，柿タンニンのみが有効であった（図1B）。ヒトノロウイルスの代替ウイルスに対しては，ネコカリシウイルスにおいて柿タンニンをはじめとする3種類のタンニン（柿タンニン，ワットルタンニン，緑茶タンニン）で効果があったが，ネズミノロウイルスでは柿タンニンのみが有効であった（図1C，D）。

12種類すべてのウイルスに対する7種類のタンニン類の効果を総当たりで試験した結果を表1にまとめた。表の中の数字は試薬処理による対数の減少値を示し，有効を示す4以上は下線と太字で強調した。

一見して，エンベロープウイルス（表1の上半分）では，全般にタンニン類に感受性が高いことがわかる。これに対して，非エンベロープウイルス（表1の下半分）では，効きがよくないことがわかる。特に，コクサッキーウイルス，アデノウイルス，マウスノロウイルスは柿渋以外では不活化できず，丈夫なウイルスであると

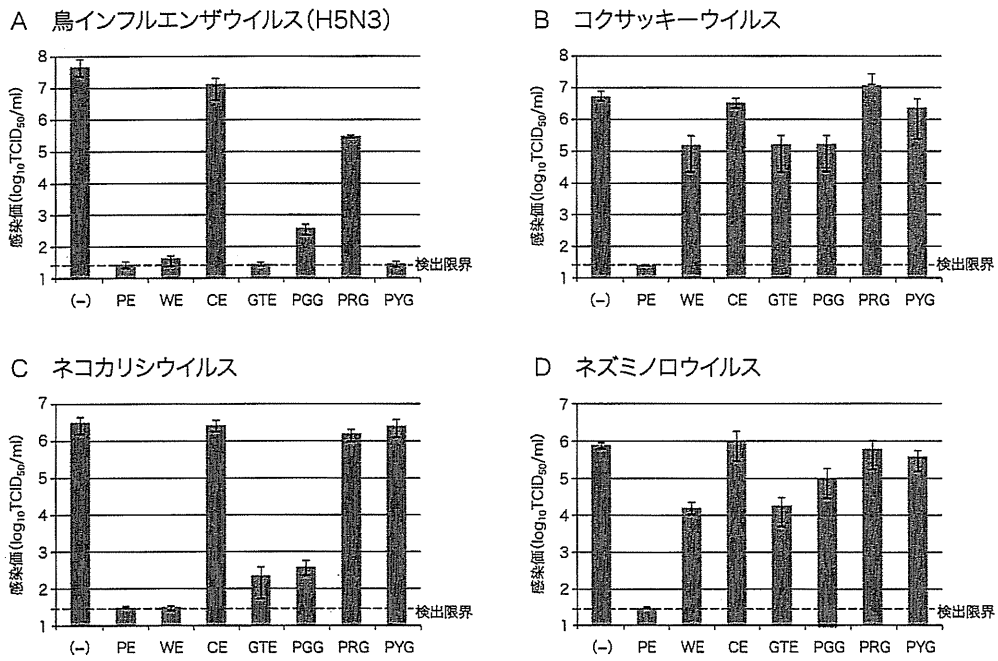


図1 ネコカリシウイルスに対するタンニン類の効果

タンニン処理後のウイルス感染価。(−) PE：柿タンニン，WE：ワットルタンニン，CE：コーヒータンニン，GTE：緑茶タンニン，PGG：ペンタガロイルグルコース，PRG：プロピロガレート，PYG：ピロガロール

考えられる。

タンニン別にみると，柿タンニンのみが，12種類のすべてのウイルスに対して抑制効果があったことがわかる。柿タンニンは，ウイルス感染価をすべて検出限界まで低下させており，完全に効いたといっても差し支えない。これに対して，他のタンニン類にはここまでの効果はない。緑茶タンニンは，柿タンニンの次に多い9種類のウイルスに対して抗ウイルス効果を示したが，アデノウイルス，ネズミノロウイルス，コクサッキーウイルスに対しては効果がみられなかった。ワットルタンニン，ペンタガロイルグルコースはそれぞれ8種類，6種類のウイルスを不活化した。一方，コーヒータンニンはどのウイルスに対しても効果がなく，このことはコーヒータンニンの主成分がクロロゲン酸で，柿タンニンや緑茶タンニンなどのようなフラボノイド骨格をもっていないことによるのかもしれない。いずれにせよ，コーヒーを飲んでもウイルス予防には役立たない。

以上の結果から，柿タンニンには広範囲のいろいろなウイルス種に対して，高い抗ウイルス効果があることが明らかとなった。この試験とは別に，ヒト免疫不全ウイルス，RS (Respiratory Syncytial) ウイルスなど複数のウイルスも調べたが，やはり柿タンニンはこれらのウイルスを不活化した。

## 2. 柿タンニンの抗ウイルス効果の性質

柿タンニンの抗ウイルス効果の有効濃度をヒト由来インフルエンザウイルス (H3N2) で調べたところ，終濃度0.01%でも部分的に有効であった。反応時間では，柿タンニンとウイルスを混和後30秒間で効果があり，柿タンニンの抗ウイルス効果は短時間で発揮されるものと考えられる。この30秒間というのは反応を稀釈でとめるために時間的な余裕をみて表示しているが，実際にはもっと短時間で効果を出していると考えられた。

ウイルス感染実験では,通常,培養細胞を洗って,ウイルス接種液を添加して1時間置き,ウイルスを細胞に吸着させる。その後にウイルス接種液を除いて,細胞培養液と入れ替える。柿タンニンをその各段階(接種前,吸着中,接種後:図2A)に加えて,どこ段階で阻害しているかを,インフルエンザウイルスで調べたところ,明らかに柿タンニンを吸着のときに加えたときに効果がみられた(図1B)。これはセンダイウイルスを使用しても同様であった。

インフルエンザウイルス感染では,上記の細胞への吸着段階を2つに分けて考えることができる。ウイルスが細胞表面のシアル酸に結合し(接着),さらにエンドサイトーシスで細胞に取り込まれ,エンドソームの酸性のためにウイルス遺伝子の細胞質への移行(侵入)が起こる。前者の「接着」は4℃でも起こるが,「侵入」には37℃の温度が必要である。そこで温度を変えることで,これらを分けて,それぞれで柿渋を添加して効果を調べたところ,4℃のウイルスの「接着」中に柿渋を加えた場合に抗ウイルス効果があることがわかった。以上のことから,柿タンニンは,おそらくウイルスと作用して,ウイルスが細胞に接着するのを防ぐと考えられた。

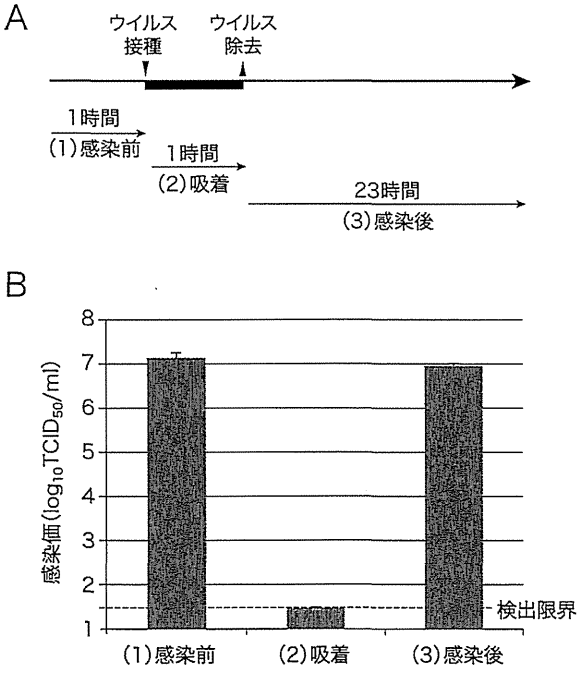


図2 (A) ウイルス感染の段階,(B) 各段階に柿渋を加えて感染実験を行い,感染後24時間後のウイルス感染価を測定した。

## 3. 抗ウイルス効果のメカニズム

このことから,柿タンニンは細胞に作用するというよりも,ウイルスに作用していると考えられた。赤血球凝集反応は,インフルエンザウイルス表面のHA(hemagglutinin:赤血球凝集素)蛋白質が,赤血球のシアル酸を含むレセプターと結合する反応であり,インフルエンザウイルスが宿主細胞に接着する現象を反映している。この反応を柿タンニンが阻害するかを検討したところ,柿タンニンとウイルスをあらかじめ混合した場合では,赤血球凝集阻止が認められた(図3)。

さらに非特異的蛋白質としてウシ血清アルブミンと柿タンニンを混合したのちに,抗ウイルス試験を行ったところ,ウシ血清アルブミンの濃度依存的に抗ウイルス効果が減弱し(図4),ウシ血清アルブミンはウイルスと競合していると考えられた。すなわち,柿タンニンは蛋白質に結合して抗ウイルス能を発揮していると考えられた。

柿タンニンとウイルス蛋白質の結合が示唆されたので,これをさらに調べるために,精製インフルエンザウイルス粒子を柿タンニンで処理し,蛋白質の電気泳動を行った。柿タンニン未処理のウイルス粒子でみられたウイルス蛋白質のバンドが,柿タンニン処理によって消失し,ゲル上部のウェル部分に蛋白質の塊が新たに現れた(図5)。このことから,柿タンニンはウイルス粒子の蛋白質と結合して巨大分子を形成し,電気泳動のゲル内に侵入できずにサンプル添加部分に引っかかっていると考えられた。対

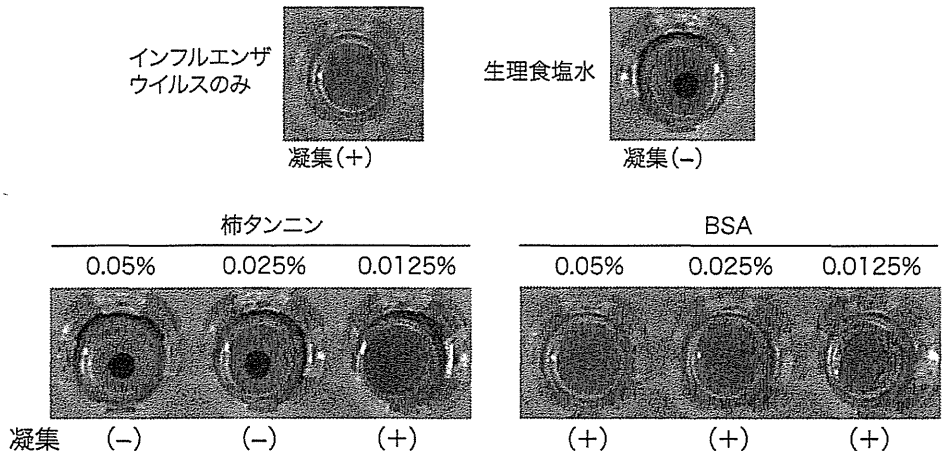


図3　柿タンニンによるインフルエンザウイルスの赤血球凝集阻止
BSA：ウシ血清アルブミン

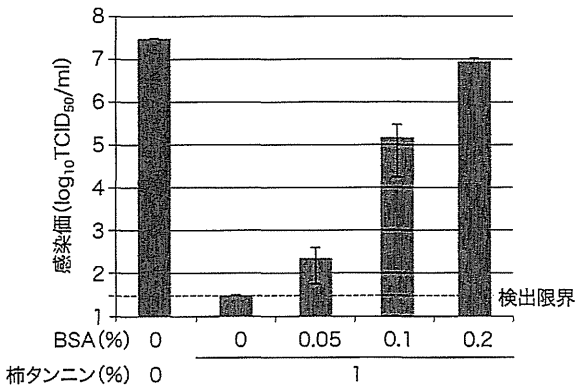


図4　ウシ血清アルブミン（BSA）による柿タンニンによる抗インフルエンザウイルス効果の阻止

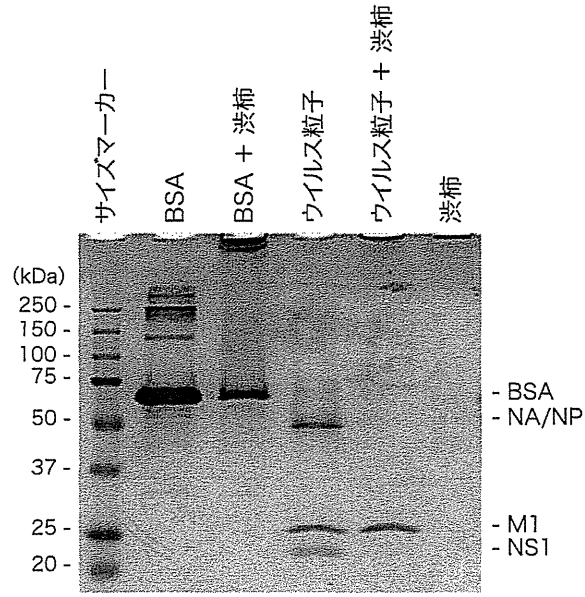


図5　蛋白質の電気泳動（SDS-PAGE）
インフルエンザウイルス粒子あるいはウシ血清アルブミン（BSA）を柿渋で処理して電気泳動を行った。NA/NP, M1, NS1 はウイルス蛋白質名である。

照としてウシ血清アルブミンを柿タンニンで処理しても，ウイルス粒子同様のことが観察された（図5）。このウイルス蛋白質の巨大分子形成が，柿タンニン以外でも起こるかどうかを調べたところ，緑茶タンニンをはじめとして他のタンニンでは，この現象はみられなかった。以前に，緑茶タンニン（カテキン）と単純ヘルペスウイルスとの凝集（巨大分子形成）が報告されているので[5]，タンニンは潜在的に，このような蛋白質凝集能があるが，本試験の条件（用いた試薬，濃度）では柿タンニンのみが巨大分子を形成したと考えられる。

以上から，柿タンニンがウイルスに結合して，言わば，立体障害によってウイルスの細胞への接着を阻止していることが考えられた。最近，柿タンニンが細菌に効果があり，それは柿タンニンによって活性酸素が産生されるためであるという論文が発表された[6]。抗ウイルス効果についても，このような機構が考えられるのかもしれない。今後の検討課題としたい。

## 4. 柿タンニンの構造と抗ウイルス効果

本研究では，ウイルス全般に対する柿タンニンの効果を示した。その中で問題となっているヒトノロウイルスに対しては，代替ウイルスとして，ネコカリシウイルスおよびネズミノロウイルスを用いて柿タンニンの有効性を示すことができた。最近，ヒトノロウイルスの遺伝子をRT-PCR法で検出することを指標として，ヒトノロウイルスを直接用いて，柿タンニンの抗ウイルス活性が示された[7]。ヒトノロウイルスには確かに効果があると考えられる。

タンニンは，加水分解を受ける芳香族カルボン酸エステルである加水分解型タンニンと，フラボノイド骨格をもつ化合物の重合体である縮合型タンニンの2種類に分類される。緑茶タンニンは加水分解型タンニンに分類され，その主成分は，エピカテキン，エピガロカテキン，エピカテキンガレート，エピガロカテキンガレートであり，それぞれが単量体として存在している。柿タンニンは縮合型タンニンに分類され，その主成分は緑茶タンニン同様4種類のカテキンであるが，それぞれが単量体として存在せず，1：1：2：2の比率で縮合した状態で存在している[8,9]。しかし，その構造は確定していない。柿タンニンと緑茶タンニンは同様の成分をもつが，その存在様式が異なる。このことが抗ウイルス試験の結果の違いに影響したと考えられる。これらカテキンは，フラボノイド骨格をもっており，これを介してウイルス蛋白質と結合することが抗ウイルス効果を出していると考えることができる。同じ骨格をもつ植物の色素であるアントシアニンにも抗ウイルス効果があることが報告されている[10]。

以前から緑茶タンニンであるカテキン類が，インフルエンザウイルスやヘルペスウイルス，ヒト免疫不全ウイルスに効果があるという報告がなされている[5,11-16]。しかし，柿タンニンの抗ウイルス能については報告がなかった。この理由として，緑茶タンニンは構造が決まっており，純品を手に入れることができるため，再現性が担保できるということがある。一方で粗精製物では再現性の保証が難しいと考える立場がある。実際に，いくつかの科学雑誌では，ある物質の抗微生物効果を検証する論文の場合，その物質が生物材料の粗精製物の場合には論文を受け付けないと投稿規定に明記してあるものがある。

柿タンニンの構造が決定されておらず，何をもって柿タンニンとするかということが明瞭ではないことは確かである。本研究で渋柿の絞り液（フリーズドライしたもの）を用いたが，これも，季節，土壌などの柿の成育条件などによって含まれる成分が変化するかもしれず，厳密な意味での再現性は担保できていない。しかし，柿タンニンの抗ウイルス効果については疑問の余地がないと考える。本試験での渋柿の絞り汁の異なるロットでも必ず効果がみられた。また，他の柿タンニン（例えば，奈良県農業試験場で作られた加水分解型の高純度柿タンニン，JAいわみ中央・島根大学の二日酔い防止ドリンク「晩夕飲力」）を用いても高い抗ウイルス効果がみられた。さらに柿の葉を用いた茶(柿の葉茶)にも抗ウイルス効果がみられた。この場合の結果は，5月に採取した葉よりも，タンニンが多い8月に採取された葉に由来する柿の葉茶に，より高い抗ウイルス効果がみられたという興味深いものであった。

柿タンニンのもとである柿渋は食品添加物でもあるので，口に入っても安全であり，食品を扱う場面でのノロウイルス対策に最適であると考えられる。例えば台所のまな板の消毒に適しているであろう。実際にエタノール製剤に柿渋を添加した消毒剤が市販され，主に業務用として飲食店の厨房，食品工場などで使用されてい

る（アルタン社「ノロエース」）。

前述の二日酔い防止ドリンクや，健康食品としてサプリメントで柿渋を摂取して，腸内にある程度の柿タンニンが存在する条件では，ノロウイルスのように腸から感染するウイルス感染を防ぐことができるのではないだろうか。なかなか実験による検証は難しいけれども，新たなノロウイルス対策になりえるかもしれないと考える。柿タンニンの構造決定や，柿タンニンの抗ウイルス効果の作用機構など今後解決すべき課題が残されている。

## 参考文献


1) Serrano, J., Puupponen-Pimia, R., Dauer, A. *et al.*: Tannins: current knowledge of food sources, intake, bioavailability and biological effects. *Mol. Nutr. Food Res.* **53** Suppl. 2: S310-S329, 2009.
2) Ueda, K., Kawabata, R., Irie, T. *et al.*: Inactivation of pathogenic viruses by plant-derived tannins: strong effects of extracts from persimmon (Diospyros kaki) on a broad range of viruses. *PLoS One* **8**(1): e55343, 2013.
3) 河野 晴也：さまよえる遺伝子 生体とウイルスのかかわり，培風館，1980.
4) Teunis, P. F., Moe, C. L., Liu, P. *et al.*: Norwalk virus: how infectious is it ? *J. Med. Virol.* **80**(8): 1468-1476, 2008.
5) Isaacs, C. E., Wen, G. Y., Xu, W. *et al.*: Epigallocatechin gallate inactivates clinical isolates of herpes simplex virus. *Antimicrob. Agents Chemother.* **52**(3): 962-970, 2008.
6) Arakawa, H., Takasaki, M., Tajima, N. *et al.*: Antibacterial activities of persimmon extracts relate with their hydrogen peroxide concentration. *Biol. Pharm. Bull.*, 2014, in press.
7) Kamimoto, M., Nakai, Y., Tsuji, T. *et al.*: Antiviral effects of persimmon extract on human Norovirus and its surrogate, bacteriophage MS2. *J. Food Sci.* **79**(5): M941-M946, 2014.
8) Matsuo, T. and Ito, S.: Mechanisms of removing astringency in persimmon fruits by carbon-dioxide treatment. 2. Chemical-structure of kaki-tannin from immature fruit of persimmon (*Diospyros-Kaki* L). *Agri. Biol. Chem.* **42**(9): 1637-1643, 1978.
9) Nakatsubo, F., Enokita, K., Murakami, K. *et al.*: Chemical structures of the condensed tannins in the fruits of Diospyros species. *J. Wood Sci.* **48**(5): 414-418, 2002.
10) Li, D., Baert, L., Uyttendaele, M. *et al.*: Inactivation of food-borne viruses using natural biochemical substances. *Food Microbiol.* **35**(1): 1-9, 2013.
11) Nakayama, M., Suzuki, K., Toda, M. *et al.*: Inhibition of the infectivity of influenza virus by tea polyphenols. *Antiviral Res.* **21**(4): 289-299, 1993.
12) Song, J. M., Lee, K. H., and Seong, B. L.: Antiviral effect of catechins in green tea on influenza virus. *Antiviral Res.* **68**(2): 66-74, 2005.
13) Song, J. M., Park, K. D., Lee, K. H. *et al.*: Biological evaluation of anti-influenza viral activity of semi-synthetic catechin derivatives. *Antiviral Res.* **76**(2): 178-185, 2007.
14) Fukuchi, K., Sakagami, H., Okuda, T. *et al.*: Inhibition of herpes simplex virus infection by tannins and related compounds. *Antiviral Res.* **11**(5-6): 285-297, 1989.
15) Nakashima, H., Murakami, T., Yamamoto, N. *et al.*: Inhibition of human immunodeficiency viral replication by tannins and related compounds. *Antiviral Res.* **18**(1): 91-103, 1992.
16) Yamaguchi, K., Honda, M., Ikigai, H. *et al.*: Inhibitory effects of (-)-epigallocatechin gallate on the life cycle of human immunodeficiency virus type 1 (HIV-1). *Antiviral Res.* **53**(1): 19-34, 2002.

JOURNAL OF VIRAL HEPATITIS
JVH

*Journal of Viral Hepatitis*, 2014, **21**, e89–e97 doi:10.1111/jvh.12240

# Human microRNA hsa-miR-1231 suppresses hepatitis B virus replication by targeting core mRNA

T. Kohno,[1,2*] M. Tsuge,[1,2,3*] E. Murakami,[1,2] N. Hiraga,[1,2] H. Abe,[1,2] D. Miki,[1,2,4] M. Imamura,[1,2] H. Ochi,[1,2,4] C. N. Hayes[1,2] and K. Chayama[1,2,4]

[1]*Department of Gastroenterology and Metabolism, Applied life sciences, Institute of Biomedical and Health sciences, Hiroshima University, Hiroshima, Japan;* [2]*Liver Research Project Center, Hiroshima University, Hiroshima, Japan;* [3]*Natural Science Center for Basic Research and Development, Hiroshima University, Hiroshima, Japan; and* [4]*Laboratory for Liver Diseases, SNP Research Center, The Institute of Physical and Chemical Research (RIKEN), Hiroshima, Japan*

*Received November 2013; accepted for publication February 2014*

SUMMARY. Pathogen-specific miRNA profiles might reveal potential new avenues for therapy. To identify miRNAs directly associated with hepatitis B virus (HBV) in hepatocytes, we performed a miRNA array analysis using urokinase-type plasminogen activator (uPA)–severe combined immunodeficiency (SCID) mice where the livers were highly repopulated with human hepatocytes and human immune cells are absent. Mice were inoculated with HBV-infected patient serum samples. Eight weeks after HBV infection, human hepatocytes were collected from liver tissues, and miRNAs were analysed using the Toray 3D array system. The effect of miRNAs on HBV replication was analysed using HBV-transfected HepG2 cells. Four miRNAs, hsa-miR-486-3p, hsa-miR-1908, hsa-miR-675 and hsa-miR-1231 were upregulated in mouse and human livers with HBV infection. These miRNAs were associated with immune response pathways such as inflammation mediated by chemokine and cytokine signalling. Of these miRNAs, hsa-miR-1231, which showed high homology with HBV core and HBx sequences, was most highly upregulated. In HBV-transfected HepG2 cells, overexpression of hsa-miR-1231 resulted in suppression of HBV replication with HBV core reduction. In conclusion, a novel interaction between hsa-miR-1231 and HBV replication was identified. This interaction might be useful in developing new therapeutic strategies against HBV.

*Keywords:* HB core, hepatitis B virus, hsa-miR-1231, human hepatocyte chimeric mouse, microRNA.

## INTRODUCTION

Hepatitis B virus (HBV) is a member of the *Hepadnaviridae* family, which contains a group of hepatotropic small DNA viruses that infect their respective animal hosts [1–3]. Once HBV infects human hepatocytes, the HBV genome translocates into the nucleus. Some genome copies are converted into a covalently closed circular DNA (cccDNA) form and organized into a minichromosome with histone and nonhistone proteins [4–8]. HBV cccDNA utilizes the cellular transcriptional machinery to produce all viral RNAs including the pregenomic RNA [9], and these gene products regulate viral replication and pathogenesis by regulating host gene expression [10,11].

MicroRNAs (miRNAs) are small noncoding RNAs of 21-25 nucleotides in length, processed from hairpin-shaped transcripts [12]. MiRNAs can bind the 3′-untranslated regions (UTRs) of messenger RNAs and downregulate gene expression by cleaving messenger RNA or inhibiting translation. Several miRNAs associated with HBV infection, HBV replication and hepatocarcinogenesis have recently been identified [13–19]. However, the direct influence of HBV infection on miRNA expression is still unclear.

MicroRNAs are currently being investigated for their therapeutic potential in antiviral therapy. As several studies have demonstrated that hsa-miR-122, which is specifically and abundantly expressed in hepatocytes, supported hepatitis C virus (HCV) replication by improving RNA

Abbreviations: HBc, hepatitis B core; HBsAg, hepatitis B surface antigen; HBV, hepatitis B virus; miRNA, microRNA; RI, replication intermediates.

Correspondence: Kazuaki Chayama, Department of Gastroenterology and Metabolism, Applied life sciences, Institute of Biomedical and Health sciences, Hiroshima University, 1-2-3 Kasumi, Minami-ku, Hiroshima-shi, Hiroshima, 734-8551, Japan.
E-mail: chayama@hiroshima-u.ac.jp
*These authors contributed equally to this work.

This study was supported in part by a Grant-in-Aid for Scientific Research from the Japanese Ministry of Labor and Health and Welfare.

stability [20–24]. small molecules or siRNAs which are able to knock down miR-122 expression have been explored as a new therapeutic agent for HCV eradication.

A similar microRNA-based antiviral approach is also sought for the treatment of chronic hepatitis B, as it is difficult to eradicate HBV genomes converted into cccDNA or minichromosomes under present antiviral therapies. To develop new strategies for complete eradication of the viral genome from hepatocytes, it is important to clarify the direct associations between hepatic miRNAs and HBV infection.

In this study, miRNA microarray analysis was performed using human hepatocyte chimeric mouse livers to assess the direct impact of HBV infection on miRNA expression. We successfully demonstrated that HBV infection attenuated the expression of miRNAs under immunodeficient conditions to protect early viral propagation. A novel interaction between hsa-miR-1231 and HBV replication was identified.

## MATERIALS AND METHODS

### *Human serum inoculum*

Serum samples were obtained from a carrier infected with HBV genotype C after obtaining written informed consent for the donation and evaluation of blood samples. Inoculum was positive for HBs and HBe antigens with high-level viremia (HBV DNA: 7.1 log copies/mL). The experimental protocol conformed to the ethical guidelines of the Declaration of Helsinki and was approved by the Hiroshima University Hospital ethical committee (Approval ID: D08-9).

### *Human hepatocyte chimeric mice experiments*

Human hepatocyte chimeric mice (PXB mice), in which human hepatocytes were transplanted into uPA$^{+/+}$/SCID$^{+/+}$ mice, were purchased from Phoenix Bio (Hiroshima, Japan). Mouse experiments were performed in accordance with the guidelines of the local committee for animal experiments at Hiroshima University.

Six chimeric mice, in which more than 90% of the liver tissue was replaced with human hepatocytes, were divided into two experimental groups. Group A contained three uninfected mice. Group B consisted of three mice that were inoculated via the mouse tail vein with human serum containing $6 \times 10^6$ copies of HBV. Serum HBV DNA titres were quantified every 2 weeks by real-time PCR, and human albumin levels were measured using the Human Albumin ELISA Quantitation kit (Bethyl Laboratories Inc., Montgomery, TX, USA) as described previously [25]. Eight weeks after inoculation, all three infected mice were sacrificed. Infection, extraction of serum samples and sacrifice were performed under ether anaesthesia as described previously [26].

### *miRNA microarray analysis*

Human hepatocytes were finely dissected from the mouse livers and stored in liquid nitrogen after submerging in RNA*later*® solution (Applied Biosystems, Foster City, CA, USA). Experimental sample RNAs were isolated using RNeasy Mini Kit (Qiagen, Valencia, CA, USA) and analysed using TORAY 3-D Gene Chip human miRNA ver. 12.1 (TORAY, Chiba, Japan).

### *Data analysis*

Gene expression profiles were analysed using GeneSpring GX 10.0.2 software (Tomy Digital Biology, Tokyo, Japan). Expression ratios were normalized per chip to the 50th percentile. To determine whether there were miRNAs differentially expressed among samples, we performed two Welch's *t*-tests ($P < 0.01$) on this prescreened list of miRNAs with Benjamini and Hochberg's correction. Complete linkage hierarchical clustering analysis was applied using Euclidean distance.

### *Pathway analysis*

The miRNA target genes were predicted by the online database miRWalk (http://www.umm.uni-heidelberg.de/apps/zmf/mirwalk/index.html). Target prediction was performed using 3′-UTR sequences of mRNAs, and the probability distributions were calculated using the Poisson distribution [27]. The mRNAs with *P* values <0.01 were considered significant. To improve the accuracy of target gene selection, the predicted genes were screened using other prediction programs, including miRanda (August 2010 release), miRDB (April 2009 release) and TargetScan version 5.1 (Whitehead Institute for Biomedical Research, Cambridge, MA, USA). Genes that were predicted by at least two alternate programs were selected. Pathway analysis was performed by PANTHER version 8.1 (http://www.pantherdb.org/) to determine the effects of the predicted target genes on pathways.

### *Quantification of miRNAs*

Small RNAs were extracted from liver tissues or HepG2 cells with mirVana™ miRNA Isolation Kit (Applied Biosystems) and reverse-transcribed according to the manufacturer's instructions. The selected miRNAs were quantified with TaqMan® MicroRNA Assays (Applied Biosystems) using the 7300 Real-Time PCR System (Applied Biosystems), and the expression of RNU6B served as a control.

### *Quantification of mRNAs*

Total RNA was extracted from HepG2 cells transfected with control miRNA or miR-1231 expression plasmid using

RNeasy Mini Kit and reverse-transcribed (RT) using ReverTra Ace (TOYOBO, Osaka, Japan) with random primer according to the manufacturer's instructions. The selected cDNAs were quantified by real-time PCR. Differences between groups were examined for statistical significance using Student's *t*-test. The primer sequences were as follows: GAPDH forward 5′-ACAACAGCCTCAAGATCATCAG-3′ and reverse 5′-GGTCCACCACTGACACGTTG-3′; Mx1 forward 5′- TTCGGCTGTTTACCAGACTCC-3′ and reverse 5′- CAAAGCCTGGCAGCTCTCTAC-3′; 2′–5′ oligoadenylate synthetase 1 (OAS1) forward 5′- ACCTGGTTGTCTTCCTCA GTCC-3′ and reverse 5′- GAGCCTGGACCTCAAACTTCAC-3′; double stranded RNA dependent protein kinase (PKR) forward 5′- TGGCCGCTAAACTTGCATATC-3′ and reverse 5′- AGTTGCTTTGGGACTCACACG-3′; and SOCS1 forward 5′-ACGAGCATCCGCGTGCACTT-3′ and reverse 5′-AAGAGG CAGTCGAAGCTCTC-3′.

### *Plasmid construction*

The construction of wild-type HBV 1.4 genome length, pTRE-HB-wt, was described previously [25]. The nucleotide sequence of the cloned HBV genome was deposited into GenBank AB206817. The HBc and HBx genes, amplified from pTRE-HB-wt, were cloned into pcDNA3 and p3xFLAG-CMV10 vectors and designated pcDNA-HBc and p3FLAG-HBx, respectively. The human miR-1231 precursor expression plasmid (HmiR0554-MR04) and the control miRNA plasmid (CmiR0001-MR01), which was a miRNA-scrambled control clone, were commercially produced (GeneCopoeia™, Rockville, MD, USA).

### *Transfection of HepG2 cell lines with the plasmids*

The HBV expression plasmid was transfected into HepG2 cells with control miRNA or miR-1231 expression plasmid using *Trans*IT-LT1 (Mirus, Madison, WI, USA) reagent according to the manufacturer's instructions. 24–48 h after transfection, core-associated HBV DNA and HBV RNA were extracted and quantified by real-time PCR or RT real-time PCR, respectively [28]. For identifying targets within the HBV genome, HBc or HBx expression plasmids were transiently transfected with miR-1231 expression plasmid into HepG2 cells. Twenty-four hours after transfection, the cells were harvested to perform Western blot analysis.

### *Analysis of HBV replication intermediates*

Quantitative analysis of HBV replication intermediates was performed as described previously [29]. The HBV-specific primers used for amplification were 5′-TTTGGGCATGGAC-ATTGAC-3′ and 5′-GGTGAACAATGTTCCGGAGAC-3′. The lower detection limit of this assay was 300 copies.

### *Western blot analysis*

Cell lysates, prepared with RIPA like buffer [50 mM Tris-HCl (pH 8.0), 0.1% SDS, 1% NP-40, 150 mM sodium chloride, and 0.5% sodium deoxycholate] containing protease inhibitor cocktail (Sigma-Aldrich, Tokyo, Japan), were separated on 5–20% (wt/v) SDS-polyacrylamide gels (Bio-Rad Laboratories, Inc., Tokyo, Japan). Immunoblotting was performed with anti-FLAG M2 monoclonal antibody (Sigma-Aldrich) or anti-HBV core monoclonal antibody HB91 (Advanced Life Science Institute Inc., Saitama, Japan) or anti β-actin monoclonal antibody (Sigma-Aldrich) followed by incubation with horseradish peroxidase-conjugated sheep anti-mouse immunoglobulin (GE Healthcare, Buckinghamshire, UK). Expression of HBc protein was quantified based on the densities of the immunoblot signals by Quantity One® software (Bio-Rad Laboratories, Inc.).

## RESULTS

### *miRNA expression alterations associated with HBV infection*

To analyse the influence of HBV infection on human hepatocytes, miRNA microarray expression profiles were compared between groups A (mice without HBV infection) and B (mice with HBV infection). Among the 900 miRNAs on the microarray, 10 miRNAs showed a more than 2.0-fold change with HBV infection. Five of the 10 miRNAs were upregulated, and the remaining five were downregulated (Fig. S1). Because immunity was severely suppressed in the chimeric mice, changes in miRNA expression are thought to be closely associated with HBV infection, and the upregulated miRNAs might play a protective role against HBV infection. Thus, we focused on these 5 upregulated miRNAs.

### *Comparison of expression of the 5 upregulated miRNAs in human liver tissues*

To verify the microarray results, quantitative analysis of miRNAs was performed using liver tissues from the chimeric mice. Three of the 5 miRNAs were significantly upregulated by HBV infection (Fig. 1). Expression changes in the other 2 miRNAs (hsa-miR-675 and hsa-miR-1908) showed a similar trend but were not significant due to individual variation. Therefore, further quantitative analysis was performed using human liver tissues. Nine liver tissue samples were obtained from patients with chronic hepatitis B ($N = 3$), chronic hepatitis C ($N = 2$) or alcoholic liver dysfunction ($N = 4$), and miRNA expression levels were compared. Expressions of all miRNAs except for miR-886-5p were significantly higher in liver tissues with chronic hepatitis B than in those with other liver diseases (Fig. 2).